iScience

CellPress
OPEN ACCESS

Article

Structure-affinity and structure-residence time relationships of macrocyclic $G\alpha_q$ protein inhibitors

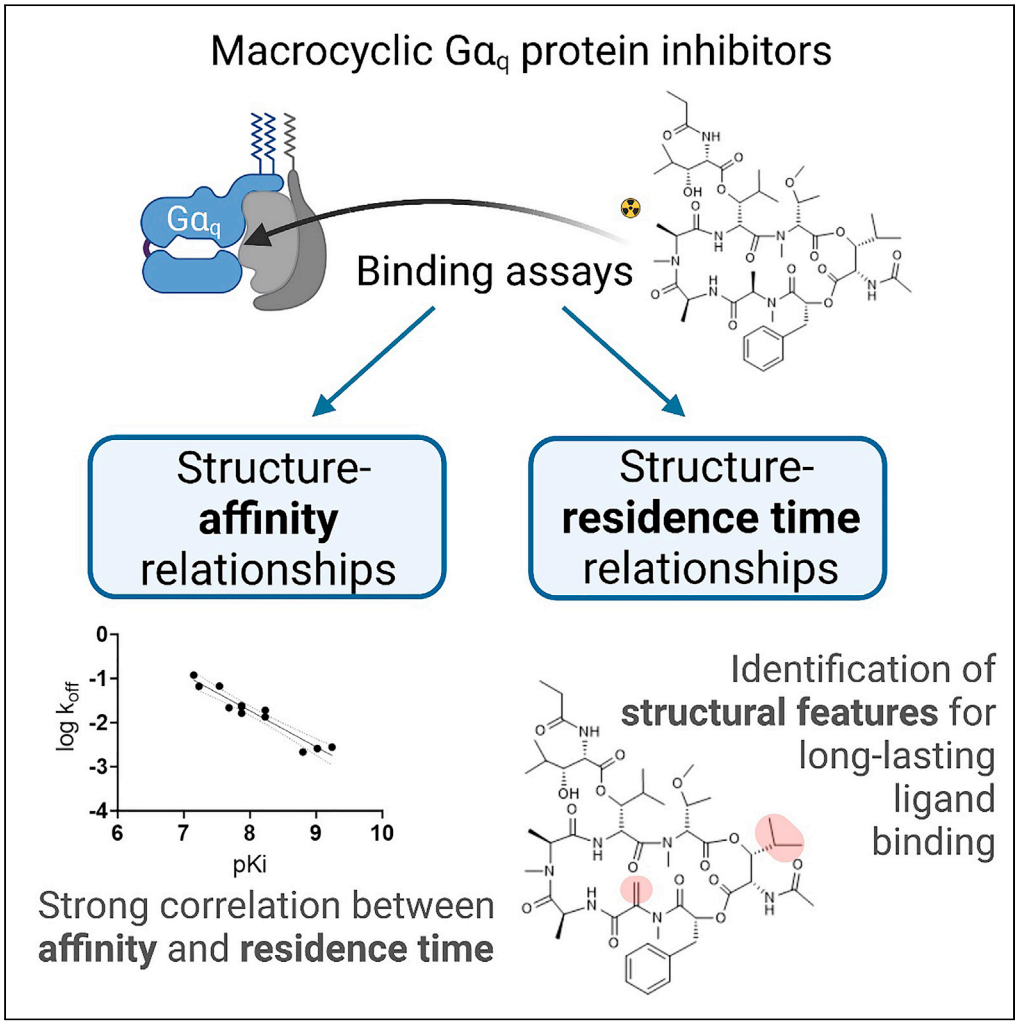

Jan H. Voss, Max Crüsemann, Christian R.O. Bartling, ..., Gabriele M. König, Kristian Strømgaard, Christa E. Müller

christa.mueller@uni-bonn.de

Highlights

Structure-affinity and -kinetics relationships of Gq protein inhibitors were studied

Small structural modifications led to drastically reduced residence times

The natural product FR900359 had a higher residence time than its hydrogenated radioligand

The isopropyl anchor present in FR900359 is crucial for ultra-long inhibitor binding

Voss et al., iScience *26*, 106492
April 21, 2023
https://doi.org/10.1016/j.isci.2023.106492

iScience

CellPress
OPEN ACCESS

Article

Structure-affinity and structure-residence time relationships of macrocyclic $G\alpha_q$ protein inhibitors

Jan H. Voss,[1] Max Crüsemann,[2] Christian R.O. Bartling,[3] Stefan Kehraus,[2] Asuka Inoue,[4] Gabriele M. König,[2] Kristian Strømgaard,[3] and Christa E. Müller[1,5,*]

SUMMARY

The macrocyclic depsipeptides YM-254890 (YM) and FR900359 (FR) are potent inhibitors of $G\alpha_{q/11}$ proteins. They are important pharmacological tools and have potential as therapeutic drugs. The hydrogenated, tritium-labeled YM and FR derivatives display largely different residence times despite similar structures. In the present study we established a competition-association binding assay to determine the dissociation kinetics of unlabeled G_q protein inhibitors. Structure-affinity and structure-residence time relationships were analyzed. Small structural modifications had a large impact on residence time. YM and FR exhibited 4- to 10-fold higher residence times than their hydrogenated derivatives. While FR showed pseudo-irreversible binding, YM displayed much faster dissociation from its target. The isopropyl anchor present in FR and some derivatives was essential for slow dissociation. These data provide a basis for future drug design toward modulating residence times of macrocyclic G_q protein inhibitors, which has been recognized as a crucial determinant for therapeutic outcome.

INTRODUCTION

Heterotrimeric guanine nucleotide-binding proteins (G proteins) consisting of α-, β-, and γ-subunits transfer extracellular signals from G protein-coupled receptors (GPCRs) to intracellular effector proteins. Upon receptor activation, the α-subunit dissociates from the βγ-subunits to induce intracellular effects, e.g., by modulating the formation of second messengers.[1,2] Four families of Gα proteins exist, designated $G\alpha_s$, $G\alpha_{i/o}$, $G\alpha_{q/11}$, and $G\alpha_{12/13}$.[3] Only few tool compounds are available that directly inhibit or activate heterotrimeric G proteins, in contrast to the large number of drug molecules modulating GPCRs.[4,5] Drugs acting on G proteins have great potential for the treatment of complex diseases, e.g., metabolic disorders, asthma, and cancer, that require the blockade of a master switch rather than a single receptor.[6–9] In the last decades, the macrocyclic depsipeptides YM-254890 (YM) and FR900359 (FR), natural products produced by bacteria, have been discovered to act as potent inhibitors of $G\alpha_{q/11}$ protein family members, namely of $G\alpha_q$, $G\alpha_{11}$, and $G\alpha_{14}$ proteins, being about 1000-fold less potent at the $G\alpha_{15}$ protein.[10–14] The macrocyclic backbone of these compounds is composed of seven building blocks: phenyllactic acid, dehydroalanine, two alanines, threonine, and two β-hydroxyleucine (β-HyLeu) residues in case of FR and only one β-HyLeu and a second threonine residue instead in case of YM (Figure 1). These building blocks are partly modified, e.g., by *O*- or *N*-methylation or acetylation. Moreover, another β-HyLeu residue is attached to the free hydroxyl group of a β-HyLeu residue of the macrocyclic core.[15] A number of analogs of YM and FR have either been extracted from the plant *Ardisia crenata*, which harbors the uncultivable FR-producing endosymbiontic bacterium *Candidatus burkholderia crenata*[16,17] and from cultures of *Chromobacterium vaccinii*[18,19] or have been prepared by total synthesis.[20–23] Up to now, most derivatives of YM and FR were exclusively evaluated in functional assays, i.e., inositol phosphate accumulation assays, calcium mobilization assays, or dynamic mass redistribution assays.[11,20–24] Data obtained by these experiments performed in living cells do not accurately reflect the affinity of the compounds to $G\alpha_{q/11}$ proteins, since they are affected by the compounds' cell membrane permeability and by the non-equilibrium assay conditions. The determination of binding affinities, e.g., by radioligand-binding assays, provides a more suitable basis for the analysis of structure-affinity relationships and subsequent drug design.[25]

[1]PharmaCenter Bonn, Pharmaceutical Institute, Pharmaceutical & Medicinal Chemistry, University of Bonn, An der Immenburg 4, D-53121 Bonn, Germany

[2]Institute of Pharmaceutical Biology, University of Bonn, Nussallee 6, 53115 Bonn, Germany

[3]Department of Drug Design and Pharmacology, Center for Biopharmaceuticals, University of Copenhagen, Universitetsparken 2, 2100 Copenhagen, Denmark

[4]Tohoku University, Graduate School of Pharmaceutical Sciences, Sendai, Miyagi 980-8578, Japan

[5]Lead contact

*Correspondence: christa.mueller@uni-bonn.de

https://doi.org/10.1016/j.isci.2023.106492

FR derivatives

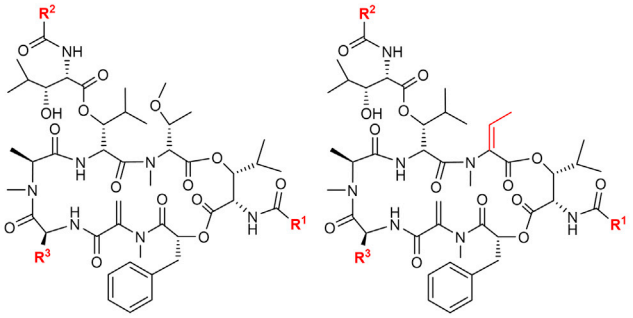

FR900359, FR-1-4 FR-6

Compound	R^1	R^2	R^3	pK_i	τ (min)
FR900359	CH_3	C_2H_5	CH_3	**8.73**	**466**
FR-1	$(CH_2)_2OH$	C_2H_5	CH_3	**8.20**	**524**
FR-2	CH_3	CH_3	CH_3	**8.74**	**547**
FR-3	C_2H_5	C_2H_5	CH_3	**7.87**	**72**
FR-4	CH_3	C_2H_5	C_2H_5	**7.87**	**72**
FR-6	CH_3	C_2H_5	CH_3	**7.25**	**n.d.**

FR- and YM-derived radioligands

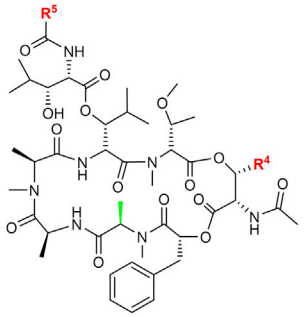

Compound	R^4	R^5	pK_D	τ (min)
[^{3}H]PSB-15900	$C(CH_3)_2$	C_2H_5	**8.19**	**131**
[^{3}H]PSB-16254	CH_3	CH_3	**7.80**	**6**

YM derivatives with modifications at the β-OH-Leu side chain

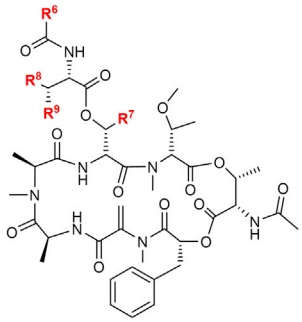

Compound	R^6	R^7	R^8	R^9	pK_i	τ (min)
YM-254890	CH_3	$CH(CH_3)_2$	$CH(CH_3)_2$	OH	**8.23**	**57**
YM-7	CH_3	$CH(CH_3)_2$	CH_3	OH	**6.45**	**n.d.**
YM-8	CH_3	CH_3	$CH(CH_3)_2$	OH	**6.43**	**n.d.**
YM-9	CH_3	$CH(CH_3)_2$	$CH(CH_3)_2$	H	**5.77**	**n.d.**
YM-10	C_2H_5	$CH(CH_3)_2$	$CH(CH_3)_2$	OH	**7.68**	**72**

YM derivatives with modifications at alanine residues or of the macrocylic core

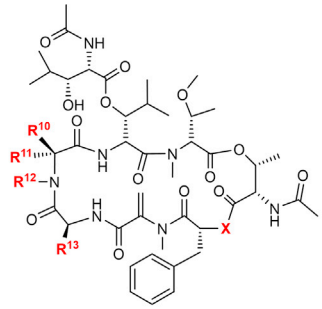

Compound	R^{10}	R^{11}	R^{12}	R^{13}	Y	pK_i	τ (min)
YM-254890	CH_3	H	CH_3	CH_3	O	**8.23**	**57**
YM-1	CH_3	H	H	CH_3	O	**6.27**	**n.d.**
YM-3	CH_3	H	CH_3	CH_3	NH	**5.57**	**n.d.**
YM-11	$CH(CH_3)_2$	H	CH_3	CH_3	O	**6.62**	**n.d.**
YM-12	H	H	CH_3	CH_3	O	**7.15**	**8**
YM-13	H	CH_3	CH_3	CH_3	O	**7.23**	**17**
YM-14	CH_2Ph	H	CH_3	CH_3	O	**7.54**	**14**
YM-15	CH_3	H	CH_3	$CH(CH_3)_2$	O	**7.02**	**n.d.**
YM-18	CH_3	H	CH_3	CH_2Ph	O	**7.88**	**55**

Figure 1. Chemical structures, affinity values (pK_i or pK_D), and residence times (τ, in min) of FR, YM, and all characterized derivatives and analogs; n.d., not determined due to low affinity. The labeling position of the radioligands was highlighted in green

In recent years, binding kinetics have emerged as a key parameter for drug molecules that is to be optimized during the drug development process. Specifically, the residence time of a drug at its target, which is determined by its unbinding kinetics, was found to play a pivotal role for the efficacy of a drug in a clinical

setting.[26–30] Despite their great importance, binding kinetics are often neglected in drug discovery, since in routinely employed assays, parameters such as IC_{50} and K_i values are determined at a single time point only.

In a previous study, we developed a radioligand-binding assay using hydrogenated derivatives of YM and FR ([^{3}H]PSB-16254 and [^{3}H]PSB-15900, respectively) that enabled the discovery of large differences in dissociation kinetics of these YM- and FR-derived radioligands: the residence time of [^{3}H]PSB-15900 (131 min at 37°C) was found to be more than 20-fold higher than that of [^{3}H]PSB-16254 (6 min at 37°C) despite the very similar structure of the two molecules (see Figure 1).[31] The different residence times could mainly be attributed to additional hydrophobic interactions between the FR-derived [^{3}H]PSB-15900 and the amino acid residues within its binding site at the $G\alpha_q$ protein as compared to the YM-derived [^{3}H]PSB-16254, as determined by a combined mutagenesis and computational approach.[32] In the present study, we determined the affinities of a broad range of FR and YM derivatives and analogs for the $G\alpha_q$ protein, which was recombinantly expressed in human embryonic kidney cells, in which the $G\alpha_{q/11}$ protein family had been knocked out. Moreover, we established an assay protocol for competition-association binding assays to investigate the binding kinetics of unlabeled compounds and to determine their residence times, enabling the establishment of structure-kinetics relationships for this promising class of potent drug molecules.

RESULTS

The binding affinities and binding kinetics of 17 macrocyclic $G\alpha_{q/11}$ protein inhibitors were determined to establish structure-affinity and, in particular, structure-residence time relationships. To this end, we employed a radioligand-binding assay using the radiolabeled FR derivative [^{3}H]PSB-15900.[31]

Characterization of binding constants

To assess the affinity and binding kinetics of unlabeled $G\alpha_{q/11}$ protein inhibitors, we initially redetermined the affinity and binding kinetics of the radiolabeled FR derivative [^{3}H]PSB-15900 at HEK293 membranes exclusively expressing the $G\alpha_q$ protein (HEK293-$G\alpha_q$ membrane preparations). This was required for further calculations of pK_i values and kinetic parameters of unlabeled compounds measured under identical conditions. In this series of experiments, we determined a pK_D value of 8.19 for [^{3}H]PSB-15900 and a maximum binding capacity (B_{max}) of 27.5 pmol per mg of protein in recombinant cell membrane preparations (Figure 2 A), which was consistent with previously published data.[32] In association experiments, an observed association rate (k_{obs}) of 0.086 min^{-1} was determined for [^{3}H]PSB-15900, resulting in a corresponding association half-life of 8.71 min (Figure 2B). Due to radioligand binding via a conformational selection mechanism, a k_{on} value cannot be reasonably calculated.[32] In dissociation experiments, a dissociation rate (k_{off}) of 0.0078 min^{-1} was determined, resulting in a dissociation half-life ($\ln(2)/k_{off}$) of 91.0 min and a residence time (τ; $1/k_{off}$) of 131 min (Figure 2C).

Binding affinities of FR and YM derivatives and analogs

Subsequently, binding affinities of FR and YM derivatives and analogs were determined by competition-binding experiments using HEK293-$G\alpha_q$ membrane preparations (Figure 3, Table 1). Due to the slow dissociation kinetics of [^{3}H]PSB-15900, all competition-binding assays were incubated for 3 h at 37°C to reach equilibrium. The isolated natural products FR and YM displayed high affinities for the $G\alpha_q$ protein (pK_i FR = 9.23, pK_i YM = 8.23), with FR being one order of magnitude more potent than YM. This is in agreement with previously described values.[31] The FR derivative FR-2 showed the same high affinity at the $G\alpha_q$ protein as FR, while FR-1 appeared to be slightly, but not significantly, less potent (pK_i FR-1 = 8.80, pK_i FR-2 = 9.02, Figure 3A). The replacement of the propionic acid side chain of FR for an acetic acid side chain in FR-2 and the hydroxyethyl side chain extension in FR-1 are thus well-tolerated modifications of FR. A 3:1 mixture of the regioisomers FR-3 and FR-4, bearing an ethyl group instead of a methyl group (FR-3 at R^1, FR-4 at R^3), was significantly less potent (pK_i FR-3/4 = 8.23, Figure 3A). Elimination of the methoxy side chain in FR-6 (pK_i = 7.26, Figure 3A) resulted in a clearly decreased binding affinity relative to the parent compound FR. The binding affinities of the radioligands [^{3}H]PSB-15900 (pK_D = 8.19) and [^{3}H]PSB-16254 (pK_D = 7.80, determined by saturation binding[32]), were found to be slightly lower (about 0.5–1 orders of magnitude) than the affinities of the parent non-hydrogenated FR (pK_i FR = 9.23) and YM (pK_i YM = 8.23), respectively.

Most of the investigated YM derivatives displayed significantly decreased affinities when compared to the parent compound YM (Figures 3B–3E). In particular, derivatives YM-1, -3, -7, -8, and -9 showed pK_i values

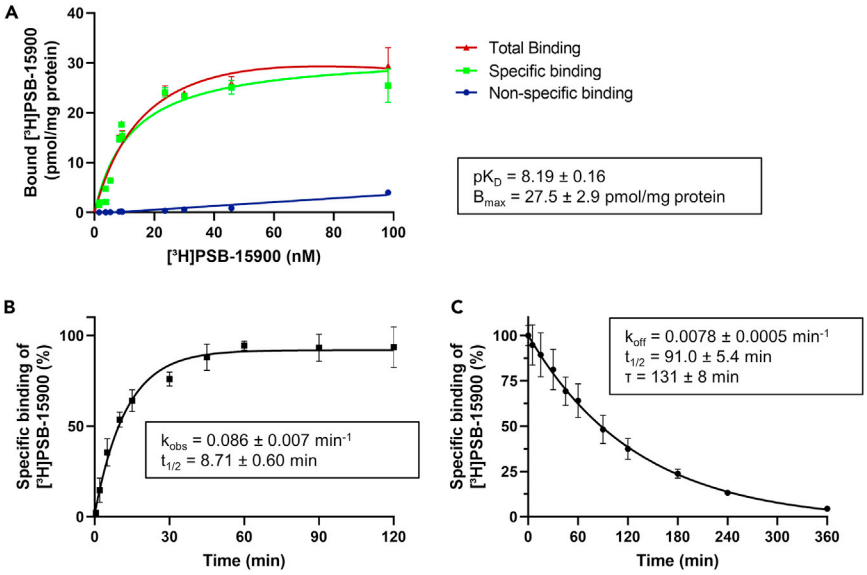

Figure 2. Binding experiments of [^{3}H]PSB-15900 to Gα_q proteins, expressed in HEK293 cell membranes

(A) Saturation binding of [^{3}H]PSB-15900 to HEK293-Gα_q membranes (25 μg of protein). The following values were determined: pK_D = 8.19 ± 0.16, B_{max} = 27.5 ± 2.9 pmol/mg.

(B) Association kinetics of [^{3}H]PSB-15900 (5 nM) to HEK293-Gα_q membrane preparations. The observed association rate k_{obs} was 0.080 ± 0.006 min-1, resulting in an association half-life (ln 2/kobs) of 8.71 ± 0.60 min.

(C) Dissociation kinetics of [^{3}H]PSB-15900 to HEK293-Gα_q membrane preparations. The dissociation rate k_{off} was determined as 0.0078 ± 0.0005 min^{-1} resulting in a dissociation half-life (ln 2/k_{off}) of 91.0 ± 5.4 min and a residence time (1/k_{off}) of 131 ± 8 min. All data points represent means ± SD of three separate experiments, performed in duplicates.

ranging from 5.57–6.45 (Figures 3B and 3C), which were much lower than those of the parent compound (pK_i YM = 8.23). The *N*-demethylation of an alanine residue in YM-1 (pK_i 6.27) resulted in an approx. 100-fold decrease in affinity compared to YM (pK_i YM = 8.23). While large parts of the contact surface between the macrocyclic Gα_q protein inhibitors and the Gα_q protein are lipophilic, a few polar interactions were found to be essential for high-affinity binding. This is demonstrated by the large loss in affinity for YM-3 (pK_i YM-3, 5.57), in which an ester bond in the macrocyclic backbone was exchanged for an amide bond, which may additionally lead to an altered conformation of the macrocycle. The exchange of an isopropyl group for a methyl group in the β-HyLeu side chain resulted in a nearly 100-fold reduction in the binding affinity for YM-7 (pK_i = 6.45) and YM-8 (pK_i = 6.43) compared to YM (pK_i YM = 8.23). Similarly, removal of the hydroxyl moiety in the side chain dramatically reduced the affinity of YM-9 (pK_i = 5.77). YM-10, which contains the propionyl residue of FR in the β-HyLeu instead of the acetyl group of YM, retained a relatively high-binding affinity (pK_i = 7.68, Figure 3C), which was, however, not significantly different from that of YM (pK_i YM = 8.23). The derivatives YM-11, -12, −13, −14, −15, and −18 contained modifications of the alanine residues of YM. They displayed high-binding affinities ranging from pK_i values of 6.62–7.88 (see Figures 3C and 3D). Exchange of the methyl group of one of the alanine residues for an isopropyl residue (YM-11), its removal (YM-12), or its steric inversion (YM-13) reduced the compounds' affinities (YM-11, pK_i = 6.62; YM-12, pK_i = 7.15; YM-13, pK_i = 7.22). Interestingly, replacing it with a benzyl side chain in YM-14 (pK_i = 7.54) did not result in a significant reduction in binding affinity compared to YM. Similarly, at the other alanine residue, replacing the methyl residue for an isopropyl group in YM-15 (pK_i = 7.02) led to a significantly reduced binding affinity, while introduction of a benzyl group in YM-18 (pK_i = 7.88) retained high affinity.

The affinity data obtained here from radioligand-binding assays showed a linear correlation with previously published potencies from functional assays (R^2 = 0.89, Figure 3F). However, pK_i values determined in binding studies were notably higher than half-maximum inhibitory concentrations (expressed as pIC_{50} values) determined in functional assays, which is especially true for the most potent inhibitors.[20–22] An explanation could be that ligand binding may not have reached equilibrium in functional assays, and therefore the potency of very potent inhibitors is likely underestimated in those studies.

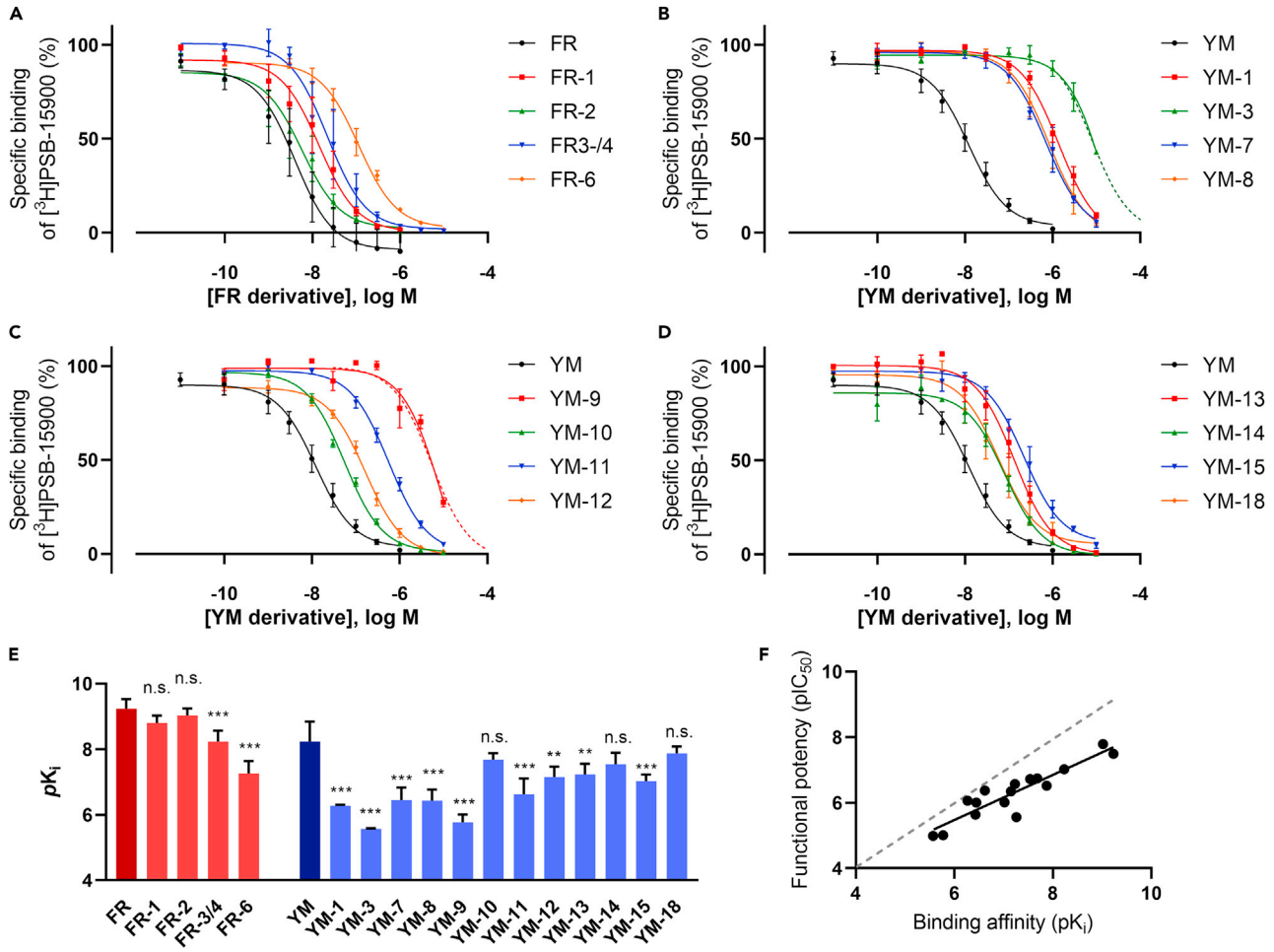

Figure 3. Characterization of FR and YM derivatives in radioligand-binding assays versus [^{3}H]PSB-15900

Competition-binding experiments of (A) FR and its derivatives, (B) YM and its derivatives YM-1, YM-3, YM-7, and YM-8, (C) YM and its derivatives YM-9 to YM-12, and (D) YM and its derivatives YM-13, YM-14, YM-15, and YM-18 versus [^{3}H]PSB-15900.

(E) pK_i values of FR, YM, and all investigated derivatives as determined in competition-binding assays. For affinity values see Table 1. Significance levels were obtained from a one-way ANOVA with multiple comparisons (FR derivatives were compared to FR, YM derivatives were compared to YM) using Dunnett's post-hoc test; $p > 0.05$ not significant (n.s.), $p < 0.05$ *; $p < 0.01$ **; $p < 0.001$ ***. Data is represented as mean ± SD of three separate experiments, performed in duplicates.

(F) Correlation of affinity data from competition-binding assays with functional data from previously performed IP_1 assays; slope = 0.75, $R^2 = 0.89$,[20–22] an ideal line (slope = 1) is plotted in light gray for comparison.

Establishment of a competition-association binding assay

As a next step, we established a competition-association binding assay to determine the binding kinetics of FR and YM derivatives. In preliminary experiments, competition-association assays were performed with 5 nM of [^{3}H]PSB-15900 and 50 nM of unlabeled FR or YM using HEK293-Gα_q membrane preparations as a Gα_q protein source (Figure 4 A). Both unlabeled competitors resulted in a large assay window. Different curve shapes for YM and FR were observed, from which dissociation rate constants could be quantified applying the model of Motulsky and Mahan.[33] When the unlabeled competitor dissociates faster from the protein than the radioligand, specific binding of the radioligand increases with time (see curve of YM vs. [^{3}H]PSB-15900 in Figure 4A). In contrast, when the competitor dissociates more slowly than the radioligand, the specific binding reaches a maximum followed by a decrease, striving toward an equilibrium (see Figure 4 A). If the kinetic properties of radioligand and competitor are essentially identical, the curve would show the shape of a one-phase association. Figure 4 A clearly shows that non-hydrogenated FR displays a slower dissociation than its respective tritiated radioligand, [^{3}H]PSB-15900, while YM displays a faster dissociation rate than [^{3}H]PSB-15900.

Table 1. Affinities of FR and YM derivatives and analogs determined in competition-binding assays versus [^{3}H]PSB-15900 compared to published potencies determined in functional assays

	Affinities ($pK_i \pm$ SD)	Published potencies (pIC_{50})
FR900359	9.23 ± 0.29	7.49[c]
FR-1	8.80 ± 0.23	n.a.
FR-2	9.02 ± 0.22	7.79
FR-3/4	8.23 ± 0.33	n.a.
FR-6	7.26 ± 0.38	5.56[d]
[^{3}H]PSB-15900	8.19 ± 0.16[a]	n.a.
YM-254890	8.23 ± 0.48	7.02[c]
YM-1	6.27 ± 0.03	6.06[c]
YM-3	5.57 ± 0.02	4.99[c]
YM-7	6.45 ± 0.38	6.00[c]
YM-8	6.43 ± 0.35	5.63[c]
YM-9	5.77 ± 0.24	5.01[c]
YM-10	7.68 ± 0.20	6.74[c]
YM-11	6.62 ± 0.48	6.38[e]
YM-12	7.15 ± 0.31	6.35[e]
YM-13	7.23 ± 0.33	6.57[e]
YM-14	7.54 ± 0.36	6.72[e]
YM-15	7.02 ± 0.20	6.01[e]
YM-18	7.88 ± 0.22	6.52[e]
[^{3}H]PSB-16254	7.80[b]	–

Affinity ata is expressed as mean ± SD from 3 to 6 independent experiments, performed in duplicate. n.a., no published data available.
[a]pK_D value determined by saturation binding.
[b]pK_D value determined by saturation binding.[32]
[c]determined by IP_1 accumulation assays.[22]
[d]determined by dynamic mass redistribution.[19]
[e]determined by IP_1 accumulation assays.[20]

Next, we determined appropriate competitor concentrations for measuring kinetic rate constants; while the radioligand concentration was kept constant at 5 nM, three different competitor concentrations, 1-, 3-, and 10-fold of the IC_{50} value (Figures 4B–4D) of FR, YM, and the high-affinity YM derivative YM-18 were employed. A 3- or 10-fold IC_{50} concentration of the unlabeled competitor resulted in plausible, virtually identical results, with FR displaying a much slower dissociation rate than YM and YM-18, whose dissociation rates were not significantly different from each other (Figure 4E). Dowling & Charlton had previously noted that a competitor concentration above the IC_{50} value was necessary to determine kinetic parameters for unlabeled compounds,[34] probably due to the minor effect of low inhibitor concentrations on the kinetics of radioligand binding. Thus, we decided to use a concentration corresponding to the 3-fold of the IC_{50} value for competition-association experiments, which allowed us to determine kinetic-binding parameters, while providing a large assay window for specific binding.

Competition-association binding experiments

Applying the optimized assay conditions, competition-association binding experiments were performed with $G\alpha_q$ protein inhibitors, that had shown pK_i values of >7, to establish structure-kinetics relationships (Figure 5, Table 2). We determined k_{off} values, kinetic rate indices (obtained by dividing specific binding at 15 min of incubation by specific binding at 180 min)[35] and residence times (τ, in min) (all values are listed in Table 2).

FR and its derivatives FR-1 and FR-2 displayed an extremely slow dissociation from the $G\alpha_q$ protein (Figures 5A–5C), with residence times of >400 min at 37°C, which did not differ significantly from each other. The structural modifications (extended, hydroxylated side chain R^1 in FR-1, and replacement of

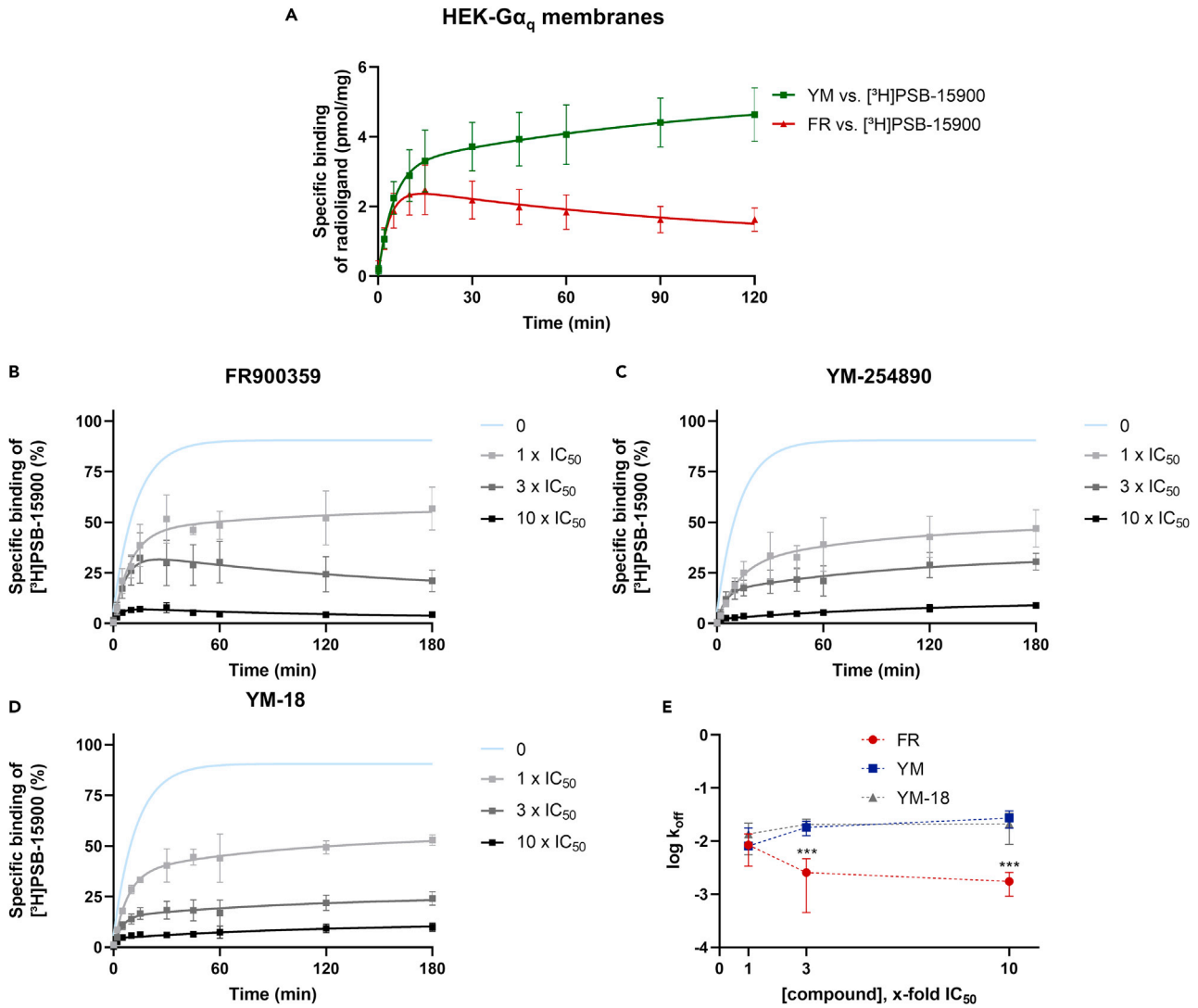

Figure 4. Establishing competition-association binding assays

(A) Competition-association binding assays with the FR-derived radioligand [^{3}H]PSB-15900 at HEK293-Gα_q membrane preparations (25 μg of protein per vial).

(B–D) Competition-association binding assays of [^{3}H]PSB-15900 versus the indicated competitor (B. FR, C. YM, D. YM-18) at 1-, 3-, and 10-fold of their IC_{50} value. The inhibitor-free association curve is displayed in light blue.

(E) The correlation between competitor concentration of FR (red), YM (blue), and YM-18 (gray) and log k_{off} as determined by the "Kinetics of competitive binding"-fit in Prism 8.4.0. All data are as means ± SD from 3 to 4 independent experiments performed in duplicates.

the propionyl by an acetyl group (R^2) in FR-2; see also Figure 1) did not affect the unbinding kinetics. As indicated by the curve shapes, all other tested compounds dissociated faster from the Gα_q protein than [^{3}H]PSB-15900. This suggests that the isopropyl group present in FR and its derivatives is pivotal for a long residence time. However, the isopropyl group is not sufficient. For instance, the mixture of FR-3/4, which both harbor ethyl groups instead of methyl groups in different positions of the backbone, dissociates from the Gα_q protein with a residence time of τ = 72 min (Figure 5D) and thus approx. 6 times faster than FR.

The parent compound YM displayed a residence time of 57 min (Figure 5E). The derivative YM-10 that contains a propionylation of the β-HyLeu side chain (like FR) instead of an acetylation like YM, displayed a slightly, but non-significantly increased residence time of 72 min (Figure 5F). YM-12, YM-13, and YM-14, all of which are modified at one of the two alanine residues of YM, dissociated fast from the Gα_q protein

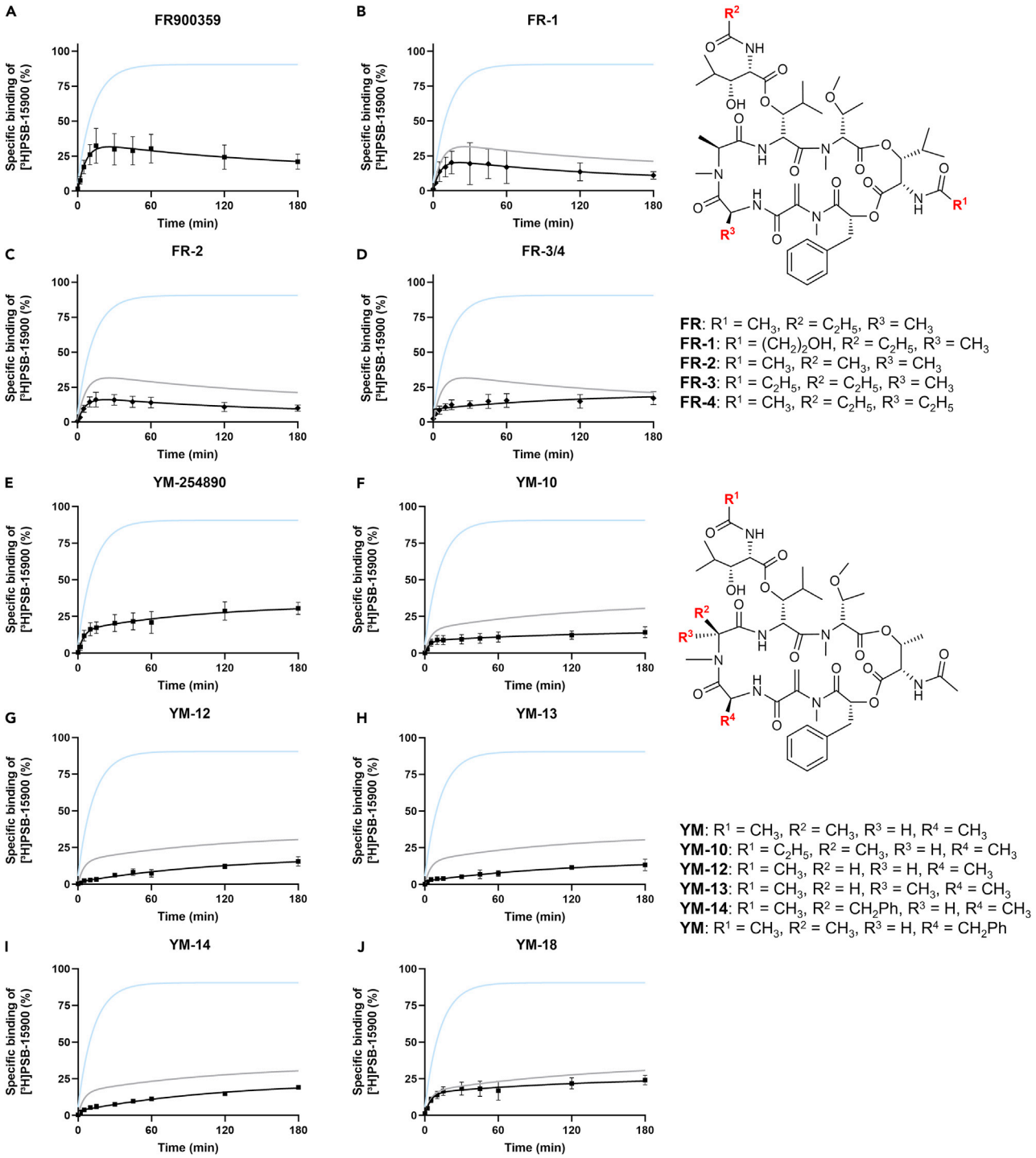

Figure 5. Competition-association assays for the determination of the residence time of $G\alpha_q$ inhibitors

The curve of the indicated compound is shown in black, the curves of competitor-free [^{3}H]PSB-15900 association are displayed in blue, and the curves of either FR (for FR-derived compounds) or YM (for YM-derived compounds) is displayed in gray for reference. A-D. Competition-association curves of FR derivatives (A. FR, B. FR-1, C. FR-2, D. FR-3/4). E-J. Competition-association curves of YM derivatives and analogs (E. YM, F. YM-10, G. YM-12, H. YM-13, I. YM-14, J. YM-18). All data are means ± SD of 3–4 independent experiments performed in duplicates.

Table 2. k_{off} values (min^{-1}), kinetic rate indices (KRI), and residence times (τ) determined for FR and YM derivatives and analogs[a]

	k_{off} (min^{-1})	Kinetic rate index (KRI)	Residence time τ (min)
[^{3}H]PSB-15900[b]	7.80 ± 0.50 × 10^{-3}	ND	131 ± 8 (**)
FR	2.56 ± 1.32 × 10^{-3}	1.62 ± 0.28	466 ± 296 ‡
FR-1	1.37 ± 0.72 × 10^{-3}	1.83 ± 0.15	524 ± 181 (n.s.)
FR-2	1.85 ± 0.15 × 10^{-3}	1.58 ± 0.12	547 ± 70 (n.s.)
FR-3/4	1.48 ± 0.24 × 10^{-2}	0.72 ± 0.03	72 ± 21 (***)
[^{3}H]PSB-16254[c]	1.77 × 10^{-1}	ND	6 (***)
YM	1.82 ± 0.22 × 10^{-2}	0.57 ± 0.03	57 ± 12 ‡
YM-10	1.50 ± 0.26 × 10^{-2}	0.62 ± 0.07	72 ± 22 (n.s.)
YM-12	1.26 ± 0.13 × 10^{-1}	0.21 ± 0.01	8 ± 2 (***)
YM-13	6.37 ± 1.29 × 10^{-2}	0.32 ± 0.04	17 ± 5 (*)
YM-14	7.35 ± 1.04 × 10^{-2}	0.32 ± 0.04	14 ± 4 (*)
YM-18	2.07 ± 0.33 × 10^{-2}	0.69 ± 0.02	55 ± 13 (n.s.)

[a]Data was obtained by competition-association assays using a 3-fold IC_{50} concentration of test compound versus 5 nM [^{3}H]PSB-15900. Values are presented as means ± SD of 3–4 independent experiments performed in duplicates; n.d. not determined. Significance levels were obtained from a one-way ANOVA with multiple comparisons (FR derivatives were compared to FR, YM derivatives were compared to YM, indicated by ‡) using Dunnett's post-hoc test; $p > 0.05$ not significant (n.s.), $p < 0.05$ *; $p < 0.01$ **; $p < 0.001$ ***.
[b]Determined by radioligand dissociation, see Figure 2.
[c]Taken from.[32]

(Figures 5G–5I). YM-18, which is benzylated at the other Ala residue of YM, shares an almost identical residence time with YM (Figure 5J).

DISCUSSION

Using a recombinant $G\alpha_q$ expression system, we derived, for the first time, structure-affinity relationships and, in particular, structure-residence time relationships for $G\alpha_q$ protein inhibitors from competition-association binding assays using the $G\alpha_q$ protein-specific radioligand [^{3}H]PSB-15900.

Structure-affinity relationships

Macrocyclic $G\alpha_q$ inhibitors bind to a cleft between the $G\alpha_q$ protein and the associated Gβ subunit (Figure 6 A); however no direct interaction with the Gβ subunit had been observed in a co-crystal structure of YM and $G\alpha_q\beta_1\gamma_2$.[31,36] The pharmacophore of the $G\alpha_q$ protein inhibitors is complex and involves all building blocks of the macrocyclic depsipeptides except for the two alanine residues that do not directly interact with the $G\alpha_q$ protein.[37] The macrocyclic $G\alpha_q$ protein inhibitors feature multiple lipophilic interactions with the wide binding pocket at the switch I/linker I region of the $G\alpha_q$ protein, and only few polar contacts, e.g., hydrogen bonds between Arg60 and the ester bond of the phenyllactic acid residue, or between the amide nitrogen of Glu191 and the free hydroxyl group of the β-HyLeu side chain. An interaction map of YM with surrounding residues is displayed in Figure 6B (see Supporting Figures S1–S4 for 2D and 3D interaction diagrams of $G\alpha_q$ protein inhibitors). It is worth noting that small modifications of the molecules can alter their conformation in solution, which might in turn also affect ligand binding to the $G\alpha_q$ protein.[38]

As previously reported based on functional assays, most modifications of the parent compounds YM and FR impaired their potency in inhibiting $G\alpha_q$ proteins.[16,20–23] In the present study, we observed that functional potencies of the macrocyclic $G\alpha_q$ protein inhibitors correlated well with their binding affinities (Figure 3 F, $R^2 = 0.89$). The potency determined in functional assays, however, was underestimated especially for high-affinity ligands, which may most likely be explained by non-equilibrium conditions in the functional studies, e.g., in inositol phosphate accumulation assays with an incubation time of only 60 min.

FR-1 (containing a hydroxypropionyl instead of an acetyl function) and FR-2 (containing a propionyl instead of an acetyl moiety at the branched β-HyLeu side chain) were found to bind to the $G\alpha_q$ protein with similar affinity

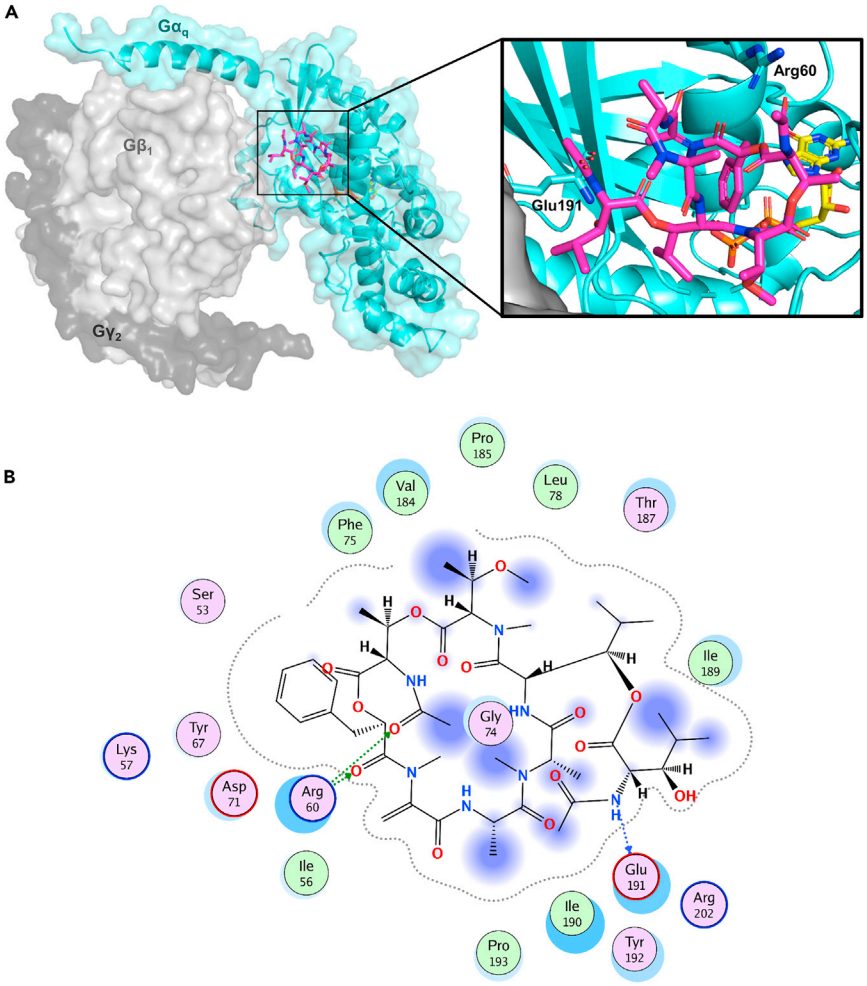

Figure 6. Binding site of macrocyclic Gα$_q$ protein inhibitors and inhibitor-protein interactions

(A) Binding site of YM (magenta) at the heterotrimeric Gα$_q$β$_1$γ$_2$ protein (Gα$_q$ cyan, Gβ$_1$ light gray, Gγ$_2$ dark gray) as determined by X-ray crystallography (PDB: 3AH8).[36] Guanosine diphosphate is shown in yellow. A close-up illustrating the binding pose of YM, highlighting the amino acids Arg60 and Glu191, at the membrane is displayed at the right.

(B) 2D-ligand interaction diagram of YM at the binding pocket of the Gα$_q$ protein, generated by Molecular Operating Environment (Chemical Computing Group, Cambridge, UK). See also Figures S1–S4 for ligand-binding site interactions of YM and FR derivatives.

as FR (*p*K$_i$ FR-1, 8.80; FR-2, 9.02; FR, 9.23). The extended side chain of FR-1 points toward the aqueous phase and likely does not interact with the Gα$_q$ protein. The truncated side chain of FR-2 is located in a rather wide pocket in proximity to Glu191 and Tyr192, which permits flexible movements of this part of the β-HyLeu side chain. The FR-3/4 mixture (3:1) displayed a significant decrease in affinity compared to FR (*p*K$_i$ FR-3/4, 8.23; *p*K$_i$ FR, 9.23). The loss of the methoxy side chain of FR-6 resulted in a significant decrease in affinity (*p*K$_i$ 7.26), presumably due to decreased contacts with a hydrophobic pocket formed by Leu78, Val182, Val184, and Pro185.

Loss of the aforementioned polar contacts between macrocyclic Gα$_q$ inhibitors and the protein resulted in a major reduction in affinity of about 2.5 orders of magnitude. This was observed for YM-3 (*p*K$_i$ YM-3, 5.57; *p*K$_i$ YM, 8.23) due to an exchange of the ester bond for an amide, which disrupts the hydrogen bond to Arg60. Similarly, YM-9 showed reduced affinity (*p*K$_i$ 5.77) due to removal of the hydroxyl group in the side chain, which disrupts hydrogen bonds with the amide of Glu191.

N-Demethylation in YM-1 (*p*K$_i$ 6.27) also resulted in an approx. 100-fold decrease in affinity, which might be explained by a conformational change in the macrocyclic backbone; the methyl group appears to point

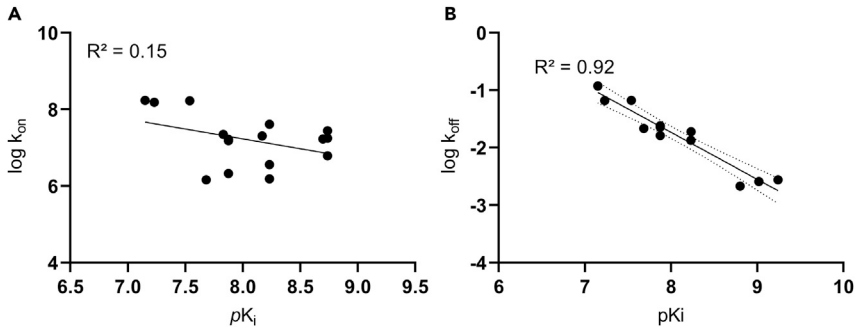

Figure 7. Correlations between affinity (pK_i) and kinetic rate constants obtained by competition-association binding assays

Correlations (A) between affinity (pK_i) and association rate (log k_{on}), and (B) between affinity (pK_i) and dissociation rate (log k_{off}). The 95%-confidence interval is shown as dotted lines in (B).

toward the solvent and does not form any significant interaction with the binding site. Other modifications of the backbone present in derivatives YM-11 to YM-15 and YM-18 were better tolerated and mostly resulted in a slight to moderate reduction in affinity (pK_i YM-11, 6.62; YM-12, 7.15; YM-13, 7.23; YM-14, 7.54; YM-15, 7.02; YM-18, 7.88). Interestingly, replacement of side chain methyl groups by isopropyl moieties in the two alanine building blocks (YM-11, YM-15) was less well tolerated as compared to the addition of a lipophilic benzyl group (YM-14, YM-18). Removal of a side chain methyl group (YM-12) or inversion of its configuration (YM-13) led to an approximately 10-fold decrease in affinity. In summary, modification of the alanine decreases the affinity of the compounds, even though these residues are expected to point to the solvent. Interestingly, only the addition of a benzyl group (YM-14, YM-18) did not result in a significant decrease in affinity relative to YM, although we did not observe new possible binding site interactions for this residue. The benzyl group, which features a flat aromatic phenyl ring, may be sterically better tolerated than a bulky isopropyl group.

In YM-7 and YM-8, isopropyl moieties within the branched β-HyLeu side chain were replaced by methyl groups, leading to reduced affinity by almost two orders of magnitude (pK_i YM-7, 6.45; YM-8, 6.43; YM, 8.23). The isopropyl group (missing in YM-7) may form lipophilic interactions with the side chains of Ile189 and Ile190, while the isopropyl group (missing in YM-8) presumably interacts with the side chains of Thr187 and Ile190. The extension of the acetyl to a propionyl residue in YM-10 was well tolerated (pK_i 7.68), which could be expected as this moiety is also present in FR and its derivatives (with the exception of FR-2).

Structure-residence time relationships

The residence time of compounds is a major determinant for the duration of their pharmacological effects; even when eliminated from the blood stream, slow-dissociating compounds may still be bound to their target. This is beneficial in some cases, where continuous inhibition of a target is essential for the pharmacological effect. For example, inhibition of airway contraction by FR, having a long residence time, in mice has previously been shown to persist for as long as 96 h after one-time intratracheal application, while effects of YM, with a significantly shorter residence time, were significantly shorter.[39] Similarly, the long-lasting effect of the muscarinic M_3 receptor antagonist tiotropium can be attributed to its slow dissociation kinetics.[40] Other diseases may in turn profit from a shorter drug residence time, e.g., fast-dissociating D_2 dopamine receptor antagonists are preferred as they still provide access for endogenous dopamine to the receptor, leading to the drugs' "atypical" antipsychotic effects.[41,42] Computational prediction models for dissociation kinetics are currently difficult to train due to the lack of structure-kinetics relationship datasets, thus the present data may be useful for establishing theoretical approaches for the estimation of residence times and the identification of key interactions required for long-lasting protein-ligand interactions.[29,43,44]

While affinity and dissociation constant correlated well, we observed no correlation between the association constant (log k_{on}) and the affinity of the compounds ($R^2 = 0.15$) (Figure 7 A). The model of Motulsky and Mahan treats ligand binding as a one-step process to a single conformation of the target protein.[33]

However, this model does not ideally fit to the binding process of YM and FR to Gα proteins: while inhibitor dissociation apparently occurs via a one-step unbinding, association involves a conformational selection step of the $G\alpha_q$ protein, which is rate-limiting for inhibitor association and renders the determination of k_{on} values based on a one-step binding model impossible.[32] Therefore, we do not consider this experimental approach valid for the determination of association rate constants of macrocyclic $G\alpha_q$ protein inhibitors. In contrast, dissociation rates (expressed as log k_{off}) and affinities (pK_i value) showed high correlation for the investigated YM and FR derivatives (R^2 = 0.92, Figure 7B). Two outliers were detected: YM dissociated faster than other compounds of similar affinity, and FR-1 (containing a hydroxypropionyl instead of an acetyl residue) displayed a longer residence time than compounds of similar affinity. The KRI, which can be determined from only two incubation time points and therefore allows a simple but nevertheless accurate estimation of the dissociation rate,[35] correlated well with log k_{off} (R^2 = 0.87, not shown).

In the present study, we were for the first time able to determine the dissociation kinetics of the natural compounds FR and YM, the highly potent $G\alpha_q$ protein inhibitors. We have observed that their hydrogenated derivatives, used as radioligands in tritiated form, [^{3}H]PSB-15900 and [^{3}H]PSB-16254, show significantly different dissociation kinetics compared to their parent, non-hydrogenated precursors (Figure 4A). Hydrogenation of the dehydroalanine residue drastically shortened the residence time of both radioligands (τ FR = 466 min vs. τ [^{3}H]PSB-15900 = 131 min, ~4-fold difference; τ YM = 57 min vs. τ [^{3}H]PSB-16254-YM = 6 min,[31] ~10-fold difference). The electron-rich C=C-bond may undergo π-π interactions with the proximate Tyr192 of the $G\alpha_q$ protein. Furthermore, the different conformations of an sp^2-and sp^3-hybridized carbon atom at this position might change the backbone conformation of the molecule. Thus, due to their strongly differing dissociation kinetics, it is not adequate to treat the parent compounds and their derived radioligands as equivalent.

The residence time τ of FR-1 and FR-2 (524 min and 547 min, respectively) is slightly but non-significantly different from that of the parent compound FR (τ FR, 466 min). This implies that the prolonged residence time of FR compared to YM is not caused by the propionyl group present in FR (replaced by an acetyl group in YM and FR-2; see R^2, R^5, R^6 in Figure 1, previously termed lipophilic "anchor 1"),[32] but by the isopropyl moiety at the core of FR (R^4 in Figure 1, "anchor 2").[32] Consistent with this finding, exchange of the acetyl group ("anchor 1") for a propionyl residue in YM-10 prolonged the residence time of YM only by approx. 25% (τ YM-10, 72 min vs. τ YM, 57 min). The 3:1 mixture of FR-3 and FR-4 dissociated significantly faster from the $G\alpha_q$ protein than the parent compound (τ FR-3/4 = 72 min vs. τ FR = 466 min). Larger ethyl instead of methyl groups thus accelerated ligand dissociation from the $G\alpha_q$ protein.

Among the YM derivatives and analogs, only YM-10 (see above), YM-12, YM-13, YM-14, and YM-18 displayed sufficiently high affinities to allow for competition-association studies. Removing a methyl group of an alanine building block (YM-12) reduced the residence time drastically from 57 min (YM) to 8 min (YM-12). Inverting its configuration (YM-13) or extending the methyl group to a benzyl group (YM-14) resulted in similar residence times of 17 and 14 min, respectively. Replacing the methyl group R^{13} with a benzyl group had no significant effect on the residence time (τ YM-18, 55 min), as compared to YM. Even though modifications of the alanine residues were well tolerated in terms of affinity, most of them (with the exception of the addition of a benzyl group in YM-18) still resulted in notably decreased residence times.

Conclusions

Altogether, steep structure-affinity and structure-residence time relationships were observed. Affinity and dissociation kinetics (expressed as log k_{off}) displayed a very high correlation (R^2 = 0.92) (Figure 7). The longest residence times (τ > 450 min) and the highest affinities were determined for FR and its derivatives FR-1 and FR-2, which emphasizes the major contribution of the isopropyl group ("anchor 2") exclusively present in FR and its derivatives to long-lasting $G\alpha_q$ protein inhibition. Well-tolerated changes of the inhibitor structure (in terms of both affinity and residence time) are exclusively located in parts of the molecule that do not interact with the $G\alpha_q$ protein but point toward the ambient aqueous phase (e.g., in FR-1, FR-2, YM-10, YM-18; Figure 6B). However, abolishing single lipophilic contacts resulted in major decreases in affinity and residence time (e.g., in YM-7, YM-8, YM-12). Similarly, hydrogenation of the double bond largely decreases the compounds' residence time (comparing YM and FR with their respective hydrogenated radioligands, Figure 4A) and (slightly) lowered their affinity (saturation pK_D of [^{3}H]PSB-15900, 8.19;

competition pK_i of FR, 9.23; saturation pK_D of [^{3}H]PSB-16254-YM, 7.80; competition pK_i of YM, 8.23). Affinity values determined by competition-binding experiments may, however, even underestimate the real affinity of very slow-dissociating compounds such as FR, FR-1, and FR-2, which would require extremely long incubation times to reach equilibrium due to their pseudo-irreversible binding to the $G\alpha_q$ protein.[32] Despite the potentially reactive partial structure (Michael acceptor) present in YM and FR, this and previous studies clearly demonstrated reversible binding of both compounds to the $G\alpha_q$ protein.[11,31]

Increasing the lipophilicity of the molecules does not necessarily result in higher affinity or longer residence time as shown by the reduced affinity of FR-3/4, YM-11, and YM-15 (see Table 2). In a previous study we have shown that many single-residue mutations greatly accelerated dissociation of YM- and FR-derived radioligands from the $G\alpha_q$ protein.[32] Combined with the present findings, we conclude that the long-lasting inhibition of $G\alpha_q$ proteins by FR is based on a network of interactions, which is easily disturbed by any modifications to the inhibitors or the protein. These data obtained in the present study provide a basis for future drug design of macrocyclic $G\alpha_q$ protein inhibitors with a long residence time, which we consider beneficial in therapeutic scenarios involving $G\alpha_q$ protein inhibitors.

Limitations of the study

This study aims at delineating the structure-affinity and especially the structure-residence time relationship of macrocyclic $G\alpha_q$ protein inhibitors. To this end, we performed competition binding and competition-association binding assays. One of the limitations of this study is due to the two-step conformational selection-binding mechanism of the investigated compounds to their target.[32] This renders the determination of k_{on} values impossible, since the rate-limiting step for ligand binding is a conformational change of the target protein which occurs before the ligand will bind.[32] Therefore, kinetic K_D values of the investigated compounds cannot be reliably calculated and compared to K_i values determined by competition binding or to K_D values determined by saturation binding experiments. Another limitation is that some of the K_i values determined for slow-dissociating inhibitors may be underestimated despite the 3-h incubation period applied in this study. But due to the very long residence times of some of the inhibitors, incubation times required to fully reach equilibrium might extend 24 h and are experimentally unfeasible. However, none of these limitations will affect the residence time determination of the $G\alpha_q$ protein inhibitors, which was the main aim of this study.

STAR★METHODS

Detailed methods are provided in the online version of this paper and include the following:

- KEY RESOURCES TABLE
- RESOURCE AVAILABILITY
  - Lead contact
  - Materials availability
  - Data and code availability
- EXPERIMENTAL MODEL AND SUBJECT DETAILS
  - Cell culture
  - Cell membrane preparation
- METHOD DETAILS
  - Saturation binding assays
  - Competition binding assays
  - Kinetic binding experiments
- QUANTIFICATION AND STATISTICAL ANALYSIS

SUPPLEMENTAL INFORMATION

Supplemental information can be found online at https://doi.org/10.1016/j.isci.2023.106492.

ACKNOWLEDGMENTS

This study was supported with a research grant from the Deutsche Forschungsgemeinschaft (FOR2372; MU1665/7-2), the Open Access Publication Fund of the University of Bonn, and the Bonn International Graduate School of Drug Sciences. A.I. was funded by the Japan Society for the Promotion of Science

(JSPS) KAKENHI grants 21H04791, 21H05113 and JPJSBP120213501, and the Japan Science and Technology Agency (JST) grant JPMJFR215T.

AUTHOR CONTRIBUTIONS

Investigation: J. H. V., formal analysis: J. H. V., methodology: J. H. V. and C. E. M., resources: M. C., C. R. O. B., S. K., G. K., K. S., writing—original draft: J. H. V. and C. E. M., writing—review and editing: J. H. V. and C. E. M. with input from all authors, visualization: J. H. V., project administration: C. E. M., funding acquisition: C. E. M. All authors have read and agreed to the published version of the manuscript.

DECLARATION OF INTERESTS

The authors declare no competing interests.

Received: January 21, 2023
Revised: February 2, 2023
Accepted: March 21, 2023
Published: March 23, 2023

REFERENCES

1. Sprang, S.R. (2016). Invited review: activation of G proteins by GTP and the mechanism of Gα-catalyzed GTP hydrolysis. Biopolymers *105*, 449–462. https://doi.org/10.1002/bip.22836.

2. Oldham, W.M., and Hamm, H.E. (2008). Heterotrimeric G protein activation by G-protein-coupled receptors. Nat. Rev. Mol. Cell Biol. *9*, 60–71. https://doi.org/10.1038/nrm2299.

3. Simon, M.I., Strathmann, M.P., and Gautam, N. (1991). Diversity of G proteins in signal transduction. Science *252*, 802–808. https://doi.org/10.1126/science.1902986.

4. Voss, J.H., and Müller, C.E. (2022). Heterotrimeric G protein A-subunits - structures, peptide-derived inhibitors, and mechanisms. Curr. Med. Chem. *29*, 6359–6378. https://doi.org/10.2174/0929867329666220308112424.

5. Hauser, A.S., Attwood, M.M., Rask-Andersen, M., Schiöth, H.B., and Gloriam, D.E. (2017). Trends in GPCR drug discovery: new agents, targets and indications. Nat. Rev. Drug Discov. *16*, 829–842. https://doi.org/10.1038/nrd.2017.178.

6. Klepac, K., Kilić, A., Gnad, T., Brown, L.M., Herrmann, B., Wilderman, A., Balkow, A., Glöde, A., Simon, K., Lidell, M.E., et al. (2016). The Gq signalling pathway inhibits brown and beige adipose tissue. Nat. Commun. *7*, 10895. https://doi.org/10.1038/ncomms10895.

7. Chua, V., Lapadula, D., Randolph, C., Benovic, J.L., Wedegaertner, P.B., and Aplin, A.E. (2017). Dysregulated GPCR signaling and therapeutic options in uveal melanoma. Mol. Cancer Res. *15*, 501–506. https://doi.org/10.1158/1541-7786.MCR-17-0007.

8. Lapadula, D., Farias, E., Randolph, C.E., Purwin, T.J., McGrath, D., Charpentier, T.H., Zhang, L., Wu, S., Terai, M., Sato, T., et al. (2019). Effects of oncogenic $G\alpha_q$ and $G\alpha_{11}$ inhibition by FR900359 in uveal melanoma. Mol. Cancer Res. *17*, 963–973. https://doi.org/10.1158/1541-7786.MCR-18-0574.

9. Kostenis, E., Pfeil, E.M., and Annala, S. (2020). Heterotrimeric Gq proteins as therapeutic targets? J. Biol. Chem. *295*, 5206–5215. https://doi.org/10.1074/jbc.REV119.007061.

10. Takasaki, J., Saito, T., Taniguchi, M., Kawasaki, T., Moritani, Y., Hayashi, K., and Kobori, M. (2004). A novel $G\alpha_{q/11}$-selective inhibitor. J. Biol. Chem. *279*, 47438–47445. https://doi.org/10.1074/jbc.M408846200.

11. Schrage, R., Schmitz, A.-L., Gaffal, E., Annala, S., Kehraus, S., Wenzel, D., Büllesbach, K.M., Bald, T., Inoue, A., Shinjo, Y., et al. (2015). The experimental power of FR900359 to study Gq-regulated biological processes. Nat. Commun. *6*, 10156. https://doi.org/10.1038/ncomms10156.

12. Gao, Z.-G., and Jacobson, K.A. (2016). On the selectivity of the Gαq inhibitor UBO-QIC: a comparison with the Gαi inhibitor pertussis toxin. Biochem. Pharmacol. *107*, 59–66. https://doi.org/10.1016/j.bcp.2016.03.003.

13. Kukkonen, J.P. (2016). G-protein inhibition profile of the reported Gq/11 inhibitor UBO-QIC. Biochem. Biophys. Res. Commun. *469*, 101–107. https://doi.org/10.1016/j.bbrc.2015.11.078.

14. Malfacini, D., Patt, J., Annala, S., Harpsøe, K., Eryilmaz, F., Reher, R., Crüsemann, M., Hanke, W., Zhang, H., Tietze, D., et al. (2019). Rational design of a heterotrimeric G protein α subunit with artificial inhibitor sensitivity. J. Biol. Chem. *294*, 5747–5758. https://doi.org/10.1074/jbc.RA118.007250.

15. Hermes, C., König, G.M., and Crüsemann, M. (2021). The chromodepsins - chemistry, biology and biosynthesis of a selective Gq inhibitor natural product family. Nat. Prod. Rep. *38*, 2276–2292. https://doi.org/10.1039/d1np00005e.

16. Reher, R., Kuschak, M., Heycke, N., Annala, S., Kehraus, S., Dai, H.-F., Müller, C.E., Kostenis, E., König, G.M., and Crüsemann, M. (2018). Applying molecular networking for the detection of natural sources and analogues of the selective Gq protein inhibitor FR900359. J. Nat. Prod. *81*, 1628–1635. https://doi.org/10.1021/acs.jnatprod.8b00222.

17. Crüsemann, M., Reher, R., Schamari, I., Brachmann, A.O., Ohbayashi, T., Kuschak, M., Malfacini, D., Seidinger, A., Pinto-Carbó, M., Richarz, R., et al. (2018). Heterologous expression, biosynthetic studies, and ecological function of the selective Gq-signaling inhibitor FR900359. Angew. Chem. Int. Ed. Engl. *57*, 836–840. https://doi.org/10.1002/anie.201707996.

18. Hermes, C., Richarz, R., Wirtz, D.A., Patt, J., Hanke, W., Kehraus, S., Voß, J.H., Küppers, J., Ohbayashi, T., Namasivayam, V., et al. (2021). Thioesterase-mediated side chain transesterification generates potent Gq signaling inhibitor FR900359. Nat. Commun. *12*, 144. https://doi.org/10.1038/s41467-020-20418-3.

19. Hanke, W., Patt, J., Alenfelder, J., Voss, J.H., Zdouc, M.M., Kehraus, S., Kim, J.B., Grujičić, G.V., Namasivayam, V., Reher, R., et al. (2021). Feature-based molecular networking for the targeted identification of Gq-inhibiting FR900359 derivatives. J. Nat. Prod. *84*, 1941–1953. https://doi.org/10.1021/acs.jnatprod.1c00194.

20. Zhang, H., Xiong, X.-F., Boesgaard, M.W., Underwood, C.R., Bräuner-Osborne, H., and Strømgaard, K. (2017). Structure-activity relationship studies of the cyclic depsipeptide natural product YM-254890, targeting the G_q protein. ChemMedChem *12*, 830–834. https://doi.org/10.1002/cmdc.201700155.

21. Zhang, H., Nielsen, A.L., Boesgaard, M.W., Harpsøe, K., Daly, N.L., Xiong, X.-F., Underwood, C.R., Haugaard-Kedström, L.M., Bräuner-Osborne, H., Gloriam, D.E., and Strømgaard, K. (2018). Structure-activity relationship and conformational studies of the natural product cyclic depsipeptides YM-254890 and FR900359. Eur. J. Med. Chem.

156, 847–860. https://doi.org/10.1016/j.ejmech.2018.07.023.

22. Xiong, X.-F., Zhang, H., Underwood, C.R., Harpsøe, K., Gardella, T.J., Wöldike, M.F., Mannstadt, M., Gloriam, D.E., Bräuner-Osborne, H., and Strømgaard, K. (2016). Total synthesis and structure-activity relationship studies of a series of selective G protein inhibitors. Nat. Chem. *8*, 1035–1041. https://doi.org/10.1038/nchem.2577.

23. Xiong, X.-F., Zhang, H., Boesgaard, M.W., Underwood, C.R., Bräuner-Osborne, H., and Strømgaard, K. (2019). Structure-activity relationship studies of the natural product Gq/11 protein inhibitor YM-254890. ChemMedChem *14*, 865–870. https://doi.org/10.1002/cmdc.201900018.

24. Taniguchi, M., Suzumura, K.-I., Nagai, K., Kawasaki, T., Takasaki, J., Sekiguchi, M., Moritani, Y., Saito, T., Hayashi, K., Fujita, S., et al. (2004). YM-254890 analogues, novel cyclic depsipeptides with Galpha(q/11) inhibitory activity from Chromobacterium sp. QS3666. Bioorg. Med. Chem. *12*, 3125–3133. https://doi.org/10.1016/j.bmc.2004.04.006.

25. Fang, Y. (2012). Ligand-receptor interaction platforms and their applications for drug discovery. Expert Opin. Drug Discov. *7*, 969–988. https://doi.org/10.1517/17460441.2012.715631.

26. Copeland, R.A., Pompliano, D.L., and Meek, T.D. (2006). Drug-target residence time and its implications for lead optimization. Nat. Rev. Drug Discov. *5*, 730–739. https://doi.org/10.1038/nrd2082.

27. Lu, H., and Tonge, P.J. (2010). Drug-target residence time: critical information for lead optimization. Curr. Opin. Chem. Biol. *14*, 467–474. https://doi.org/10.1016/j.cbpa.2010.06.176.

28. Copeland, R.A. (2016). The drug-target residence time model: a 10-year retrospective. Nat. Rev. Drug Discov. *15*, 87–95. https://doi.org/10.1038/nrd.2015.18.

29. Schuetz, D.A., de Witte, W.E.A., Wong, Y.C., Knasmueller, B., Richter, L., Kokh, D.B., Sadiq, S.K., Bosma, R., Nederpelt, I., Heitman, L.H., et al. (2017). Kinetics for drug discovery: an industry-driven effort to target drug residence time. Drug Discov. Today *22*, 896–911. https://doi.org/10.1016/j.drudis.2017.02.002.

30. van der Velden, W.J.C., Heitman, L.H., and Rosenkilde, M.M. (2020). Perspective: implications of ligand-receptor binding kinetics for therapeutic targeting of G protein-coupled receptors. ACS Pharmacol. Transl. Sci. *3*, 179–189. https://doi.org/10.1021/acsptsci.0c00012.

31. Kuschak, M., Namasivayam, V., Rafehi, M., Voss, J.H., Garg, J., Schlegel, J.G., Abdelrahman, A., Kehraus, S., Reher, R., Küppers, J., et al. (2020). Cell-permeable high-affinity tracers for Gq proteins provide structural insights, reveal distinct binding kinetics, and identify small molecule inhibitors. Br. J. Pharmacol. *177*, 1898–1916. https://doi.org/10.1111/bph.14960.

32. Voss, J.H., Nagel, J., Rafehi, M., Guixà-González, R., Malfacini, D., Patt, J., Kehraus, S., Inoue, A., König, G.M., Kostenis, E., et al. (2021). Unraveling binding mechanism and kinetics of macrocyclic Gαq protein inhibitors. Pharmacol. Res. *173*, 105880. https://doi.org/10.1016/j.phrs.2021.105880.

33. Motulsky, H.J., and Mahan, L.C. (1984). The kinetics of competitive radioligand binding predicted by the law of mass action. Mol. Pharmacol. *25*, 1–9.

34. Dowling, M.R., and Charlton, S.J. (2006). Quantifying the association and dissociation rates of unlabelled antagonists at the muscarinic M3 receptor. Br. J. Pharmacol. *148*, 927–937. https://doi.org/10.1038/sj.bjp.0706819.

35. Guo, D., van Dorp, E.J.H., Mulder-Krieger, T., van Veldhoven, J.P.D., Brussee, J., IJzerman, A.P., and Heitman, L.H. (2013). Dual-point competition association assay: a fast and high-throughput kinetic screening method for assessing ligand-receptor binding kinetics. J. Biomol. Screen *18*, 309–320. https://doi.org/10.1177/1087057112464776.

36. Nishimura, A., Kitano, K., Takasaki, J., Taniguchi, M., Mizuno, N., Tago, K., Hakoshima, T., and Itoh, H. (2010). Structural basis for the specific inhibition of heterotrimeric Gq protein by a small molecule. Proc. Natl. Acad. Sci. USA *107*, 13666–13671. https://doi.org/10.1073/pnas.1003553107.

37. Reher, R., Kühl, T., Annala, S., Benkel, T., Kaufmann, D., Nubbemeyer, B., Odhiambo, J.P., Heimer, P., Bäuml, C.A., Kehraus, S., et al. (2018). Deciphering specificity determinants for FR900359-derived Gq α inhibitors based on computational and structure-activity studies. ChemMedChem *13*, 1634–1643. https://doi.org/10.1002/cmdc.201800304.

38. Tietze, D., Kaufmann, D., Tietze, A.A., Voll, A., Reher, R., König, G., and Hausch, F. (2019). Structural and dynamical Basis of G protein inhibition by YM-254890 and FR900359: an inhibitor in action. J. Chem. Inf. Model. *59*, 4361–4373. https://doi.org/10.1021/acs.jcim.9b00433.

39. Schlegel, J.G., Tahoun, M., Seidinger, A., Voss, J.H., Kuschak, M., Kehraus, S., Schneider, M., Matthey, M., Fleischmann, B.K., König, G.M., et al. (2021). Macrocyclic Gq protein inhibitors FR900359 and/or YM-254890–fit for translation? ACS Pharmacol. Transl. Sci. *4*, 888–897. https://doi.org/10.1021/acsptsci.1c00021.

40. Barnes, P.J., Belvisi, M.G., Mak, J.C., Haddad, E.B., and O'Connor, B. (1995). Tiotropium bromide (Ba 679 BR), a novel long-acting muscarinic antagonist for the treatment of obstructive airways disease. Life Sci. *56*, 853–859. https://doi.org/10.1016/0024-3205(95)00020-7.

41. Kapur, S., and Seeman, P. (2000). Antipsychotic agents differ in how fast they come off the dopamine D2 receptors. Implications for atypical antipsychotic action. J. Psychiatry Neurosci. *25*, 161–166.

42. Vauquelin, G., Bostoen, S., Vanderheyden, P., and Seeman, P. (2012). Clozapine, atypical antipsychotics, and the benefits of fast-off D2 dopamine receptor antagonism. Naunyn-Schmiedeberg's Arch. Pharmacol. *385*, 337–372. https://doi.org/10.1007/s00210-012-0734-2.

43. Bruce, N.J., Ganotra, G.K., Kokh, D.B., Sadiq, S.K., and Wade, R.C. (2018). New approaches for computing ligand-receptor binding kinetics. Curr. Opin. Struct. Biol. *49*, 1–10. https://doi.org/10.1016/j.sbi.2017.10.001.

44. Heroven, C., Georgi, V., Ganotra, G.K., Brennan, P., Wolfreys, F., Wade, R.C., Fernández-Montalván, A.E., Chaikuad, A., and Knapp, S. (2018). Halogen-aromatic π interactions modulate inhibitor residence times. Angew. Chem. Int. Ed. Engl. *57*, 7220–7224. https://doi.org/10.1002/anie.201801666.

45. Lowry, O.H., Rosebrough, N.J., Farr, A.L., and Randall, R.J. (1951). Protein measurement with the Folin phenol reagent. J. Biol. Chem. *193*, 265–275.

STAR★METHODS

KEY RESOURCES TABLE

REAGENT or RESOURCE	SOURCE	IDENTIFIER
Chemicals, peptides, and recombinant proteins		
YM-254890	FUJIFILM Wako	253–00633
FR900359 and derivatives	S. K., M. C., G. M. K.	N/A
YM derivatives	C. R. O. B., K. S.	N/A
Experimental models: Cell lines		
HEK293-$G\alpha_q$ cells	Voss et al.[32]	N/A
Software and algorithms		
GraphPad PRISM v. 8.4	GraphPad	https://www.graphpad.com/scientific-software/prism/
ChemDraw Professional 19.1	PerkinElmer	https://www.perkinelmer.com/category/chemdraw
Other		
[^{3}H]PSB-15900	Pharmaron Ltd.	custom synthesis

RESOURCE AVAILABILITY

Lead contact

Any requests for resources and reagents used in this work shall be directed to the lead contact, Christa E. Müller (christa.mueller@uni-bonn.de).

Materials availability

This study did not generate new unique reagents.

Data and code availability

- All data reported in this paper will be shared by the lead contact upon reasonable request.
- This paper does not report original code.
- Any additional information required to reanalyze the data reported in this paper is available from the lead contact upon reasonable request.

EXPERIMENTAL MODEL AND SUBJECT DETAILS

Cell culture

Cells were cultured at 37°C and 5% CO_2 in Dulbecco's Modified Eagle Medium (DMEM) supplemented with 10% fetal calf serum, penicillin (100 U ml^{-1}), and streptomycin (0.1 mg mL^{-1}). HEK293 cells (human, female) were edited by CRISPR/Cas9 to delete the *GNAQ* and *GNA11* genes encoding the natively expressed $G\alpha_q$ and $G\alpha_{11}$ protein subunits.[11] Cells were retrovirally transfected to overexpress the human $G\alpha_q$ protein as previously described.[31,32] Transfected cells were cultured in the presence of 0.2 mg mL^{-1} G418. At 70% confluency, cells were passaged by trypsination. Routine checks for mycoplasma contamination (detection by polymerase chain reaction (PCR)) were consistently negative.

Cell membrane preparation

Recombinant HEK293 cells were seeded into cell culture dishes and incubated until confluency. The medium was discarded and the cells were frozen at −20°C overnight. The next day, cells were thawed, detached with a rubber scraper, and harvested after adding 2 mL of 5 mM Tris-HCl buffer containing 2 mM Na-EDTA, pH 7.4, per dish. The suspension was subsequently homogenized using an UltraTurrax (IKA Labortechnik, Staufen, Germany) for 1 min at level 4. Cell debris and nuclei were removed by a 10 min

centrifugation at 1,000 *g*; the pellet (P1) was discarded. The supernatant (S1) was then centrifuged again for 1 h at 48,000 *g*, the pellet (P2) was resuspended and washed with 50 mM Tris-HCl buffer, pH 7.4, and then again centrifuged for 1 h at 48,000 *g*. After discarding the supernatant, the pellet was resuspended in 50 mM Tris-HCl buffer, pH 7.4, and aliquots were stored at −80°C until use.

METHOD DETAILS

Saturation binding assays

Affinity (K_D) and maximum binding capacity (B_{max}) of the radiolabeled FR derivative [^{3}H]PSB-15900 were determined by saturation binding experiments. All binding assays employed a Tris-HCl buffer of pH 7.4, and experiments were performed in a total volume of 200 µL per sample. A series of different concentrations of [^{3}H]PSB-15900 were co-incubated with HEK293 cell membranes expressing the Gα_q protein (25 µg of protein). Unlabeled FR (final concentration: 5 µM) was used to assess non-specific radioligand binding. All samples contained a final dimethyl sulfoxide (DMSO) concentration of 2.5%. Incubation was performed for 3 h at 37°C and was terminated by rapid vacuum filtration through GF/C glass fiber filters. Filters were washed three times with 3.5 mL of ice-cold Tris-HCl buffer, pH 7.4, supplemented with 0.1% bovine serum albumin (BSA) and 0.1% of Tween 20. Filters were then transferred to scintillation vials and incubated with 2.5 mL of scintillation cocktail (LumaSafe) for 9 h before being counted in a liquid scintillation counter at 53–55% counting efficiency.

To determine K_D and B_{max} values, non-specific binding was subtracted from total binding to calculate specific binding of the radioligand. K_D and B_{max} values were calculated from the "Saturation binding: One site – specific binding" equation implemented in GraphPad Prism 8.4.0 (GraphPad, San Diego, CA, USA). Data are presented in pmol of bound radioligand per mg of protein, determined by the method of Lowry.[45]

Competition binding assays

The binding affinity of macrocyclic Gα_q inhibitors was determined by competition binding assays. A range of concentrations of test compound, dissolved in DMSO, was co-incubated with radioligand (5 nM) and HEK293 Gα_q membrane preparations (25 µg protein) for 3 h at 37°C. All other assay components were identical to those used in saturation binding assays. Samples were harvested and evaluated as described in section 2.4.

Raw data were normalized to total binding (DMSO control) = 100% and non-specific binding (5 µM of unlabeled FR) = 0%. K_i values and IC_{50} values were determined by the respective equations ("Binding – competitive: One site – Fit K_i/Fit IC_{50}). The K_D value of [^{3}H]PSB-15900, determined by saturation binding, was employed for the calculation of K_i values.

Kinetic binding experiments

In the course of this study, we performed association, dissociation, and competition-association experiments to measure the kinetics of [^{3}H]PSB-15900 as well as unlabeled compounds.

In association and competition-association experiments, membrane preparations (25 µg of protein) were added at several time points to a mixture of buffer, radioligand (5 nM), and DMSO or competitor dissolved in DMSO (final competitor concentration: 3 × IC_{50} if not mentioned otherwise, final DMSO concentration 2.5%). Non-specific binding was determined in parallel as described in the previous sections. The maximum incubation period was 3 h at 37°C. Incubation was performed upon gentle shaking.

In dissociation experiments, radioligand, protein, and buffer were pre-incubated for 1 h at 37°C (approx. 5 times the association half-life in absence of any competitor). Subsequently, an excess of unlabeled FR (final concentration: 5 µM) was added to the samples at several time points during the incubation period of 6 h at 37°C.

Samples were harvested and counted as described in section 2.4. For association and dissociation experiments, data was normalized (non-specific binding = 0%, highest cpm = 100%) and fit to a single exponential association function or an exponential decay function, respectively, to retrieve the observed association

rate constant k_{obs} and the dissociation rate k_{off}. Half-lives ($t_{1/2}$) were calculated by the equation ln (2)/k; residence time (τ) corresponds to $1/k_{off}$.

Association binding experiments were fit to a simple one-phase exponential function and analyzed only with regard to the observed association rate k_{obs}. For competition-association binding experiments, the "Kinetics of competitive binding"-fit was employed according to the model of Motulsky and Mahan.[33] B_{max} and k_{off} were constrained at experimentally determined values from saturation and dissociation binding experiments. On-rates of the radioligand were left unconstrained due to binding via a two-step conformational selection binding mechanism, which cannot be accounted for mathematically during the determination of the on-rate. On- and off-rates of the unlabeled compound were left unconstrained. For dissociation experiments, data was fit to a one-phase exponential decay model after subtraction of non-specific binding and normalization (0% = 0 cpm, 100% = highest cpm) to obtain k_{off} values and dissociation $t_{1/2}$.

QUANTIFICATION AND STATISTICAL ANALYSIS

All data points were obtained in three or more replicate experiments, each performed in duplicates (the exact number of experiments (n) is given in the figure legends). Data is presented as mean $\pm$ SD unless otherwise noted. Statistical comparisons between two values were performed by an unpaired *t*-test, comparisons between more than two mean values were carried out by a one-way analysis of variance (ANOVA) followed by Dunnett's post-hoc test. Significance levels were determined according to p values as follows: $p < 0.05$, $p < 0.01$ (**), $p < 0.001$ (***).